≪Research Paper≫ Applied Science and Convergence Technology Vol.24 No.3, May 2015, pp.67~71
http://dx.doi.org/10.5757/ASCT.2015.24.3.67

Optical Properties of InP/InGaP Quantum Structures Grown by a Migration Enhanced Epitaxy with Different Growth Cycles

Jae Won Oh[a], Il-Wook Cho[a], Mee-Yi Ryu[a]*, and Jin Dong Song[b]

[a]*Department of Physics, Kangwon National University, Chuncheon 200-701*
[b]*Center for Opto-Electronic Convergence Systems, Korea Institute of Science and Technology, Seoul 136-791*

(Received May 11, 2015, Accepted May 28, 2015)

InP/InGaP quantum structures (QSs) were grown on GaAs (001) substrates by a migration-enhanced molecular beam epitaxy method. Temperature-dependent photoluminescence (PL) and emission wavelength-dependent time-resolved PL (TRPL) were performed to investigate the optical properties of InP/InGaP QSs as a function of migration enhanced epitaxy (MEE) growth cycles from 2 to 8. One cycle for the growth of InP QS consists of 2-s In and 2-s P supply with an interruption time of 10 s after each source supply. As the MEE growth cycle increases from 2 to 8, the PL peak is redshifted and exhibited different (larger, comparable, or smaller) bandgap shrinkages with increasing temperature compared to that of bulk InP. The PL decay becomes faster with increasing MEE cycles while the PL decay time increases with increasing emission wavelength. These PL and TRPL results are attributed to the different QS density and size/shape caused by the MEE repetition cycles. Therefore, the size and density of InP QSs can be controlled by changing the MEE growth cycles.

Keywords : InP, Quantum structure, Photoluminescence, Time-resolved photoluminescence

I. Introduction

Quantum structures (QSs) have been attracted much interest because of their potential device applications in laser diode, solar cells, and optical amplifiers [1–6]. InP QSs have been investigated for the development of high-power laser diodes with a lasing wavelength of less than 750 nm to use as a pumping source for the Nd:YAG laser [5–10]. Various techniques such as In-interruption growth, As-interruption growth, and migration enhanced epitaxy method have been applied for the growth of self-assembled QSs in order to control and improve areal density, size and shape, and alignment of QSs [5,9–13]. Recently, the structural and optical properties of InP/InGaP QSs grown by various growth techniques such as metal-organic vapor phase epitaxy [6,7,14], molecular beam epitaxy [9], and migration enhanced molecular beam epitaxy [5,10–12] have been performed by using atomic force microscopy (AFM), scanning electron microscopy (SEM), photoluminescence (PL), and time-resolved PL (TRPL) etc.. Rödel et al. [9] presented the size and density of InP quantum dots (QDs) controlled by introducing growth interruption during the QD growth. The optical properties of InP/InGaP QSs

* [E-mail] myryu@kangwon.ac.kr

grown by a migration enhanced epitaxy (MEE) method were significantly influenced by growth temperatures, InGaP spacer thickness, MEE repetition cycles, etc. [10,15].

In this paper, the luminescence properties of InP/InGaP quantum structures (QSs; quantum dots+ quantum dashes) grown on GaAs substrates have been investigated by using a temperature-dependent PL and emission wavelength-dependent TRPL measurements. The size and density of InP/InGaP QSs prepared by a MEE method can be adjusted by varying the number of growth cycles.

II. Experimental Details

The InP/InGaP QS samples used in this study were grown on semi-insulating GaAs substrates by a solid source molecular beam epitaxy. Prior to InP/InGaP QS growth, a 0.1-μm-thick GaAs buffer layer was grown on the GaAs substrate at 580°C. After deposition a 50 nm-thick InGaP spacer on top of GaAs buffer layer, InP/InGaP QS was grown at 480°C by a MEE method, which alternately supplies In and P sources with a growth interruption time between depositions. One cycle for the growth of InP QS is comprised of 2-s In and 2-s P supply with an interruption time of 10 s after supplying each source. The detail of the growth conditions were published in Ref. 15. The luminescence properties of InP/InGaP QSs were carried out as a function of the number of cycles from 2 to 8.

PL and TRPL measurements were carried out at temperatures ranging from 10 to 300 K. The PL measurements were made using a 325 nm of He-Cd laser. The PL signals were collected with a CCD detector (ANDOR DV420-BU2). TRPL measurements were performed using an Edinburgh Instruments FLS 920 spectrometer. The InP/InGaP samples for TRPL were excited by using a picosecond pulsed diode laser (λ=375 nm, pulse width=50 ps) and the signal was collected by using a micro-channel plate photomultiplier tube detector. The luminescence decays were measured by using a time-correlated signal photon counting system.

III. Results and Discussion

PL spectra of InP/InGaP QS samples taken at 10 K are shown in Fig. 1(a). The PL peak is steadily redshifted from 666 to 752 nm as the MEE growth cycle increases from 2 to 8. InP/InGaP QS samples grown by changing MEE growth cycle from 2 to 8 are denoted QS2, QS3, QS4, QS5, QS6, QS7, and QS8, respectively.

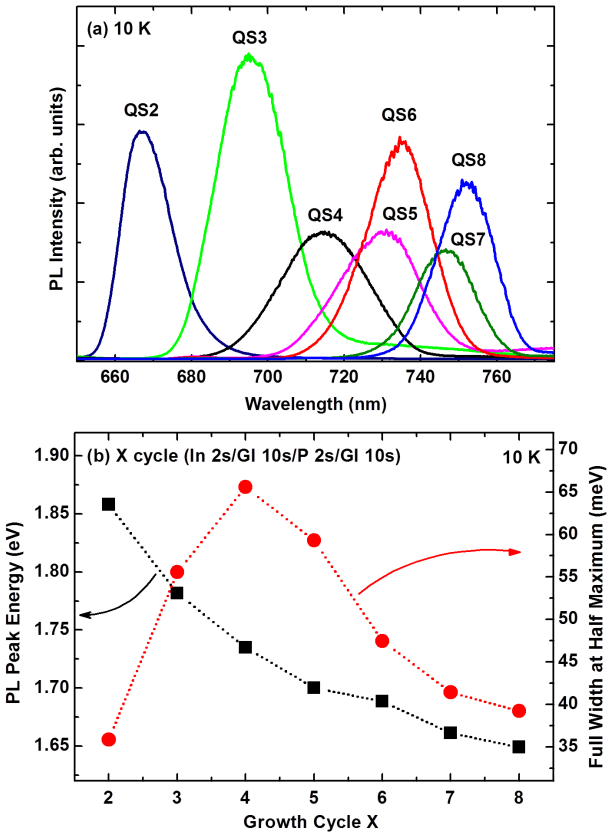

Figure 1. (a) PL spectra and (b) PL peak energy (solid squares) and full width at half maximum (solid circles) of InP/InGaP QS samples measured at 10 K as a function of the MEE growth cycles from 2 to 8.

The formation of InP/InGaP QSs was observed by the AFM and SEM, not shown here [15]. InP QDs and quantum dashes (QDash) were observed for all samples except QS2. QS2 grown by the MEE growth cycles of 2 only showed high density of QDs in the AFM and SEM images. With increasing the MEE cycles from 3 to 8, the density of QDs was reduced while the density of QDash was increased. In addition, the improved shape of QDash was obtained by the reduced length and the increased width and height as the MEE growth cycle increases from 3 to 8. Therefore, the redshift of PL peak with increasing MEE cycle is attributed to the increased size of QSs caused by enhanced indium amount as the MEE cycle increases [16].

Fig. 1(b) shows the PL peak energy (solid square) and the full width at half maximum (FWHM, solid circle) as a function of MEE growth cycle from 2 to 8. The PL peak was shifted to lower energy side from 1.86 to 1.65 eV as the MEE cycle increases from 2 to 8, respectively. The FWHM of InP QSs broadened from 36 to 66 meV with increasing the MEE cycle from 2 to 4, and then it became narrow continuously up to 39 meV up to the MEE cycles of 8 as showin in Fig. 1(b). The strongest PL intensity was obtained for QS3 sample and QS4 sample showed the most wide FWHM.

The temperature-dependent PL peak energies for QS4, QS6, and QS8 samples are shown in Fig. 2. The solid lines in Fig. 2 are the calculated temperature-dependent bandgap energies of bulk InP obtained using Varshni's equation [17]; $E_g(T)=1.421-4.9\times 10^{-4}T^2/(327+T)$ [18]. For comparison, the calculated peak position at 10 K is matched with the measured PL peak energy of each sample at 10 K. The PL peak energies of all InP/InGaP QS samples correspond with the calculated bandgap energies of bulk InP for low temperatures. At high temperatures, however, all samples exhibit different bandgap shrinkages with temperature as shown in Fig. 2. The bandgap shrinkage of QS4 sample is much fast than that of

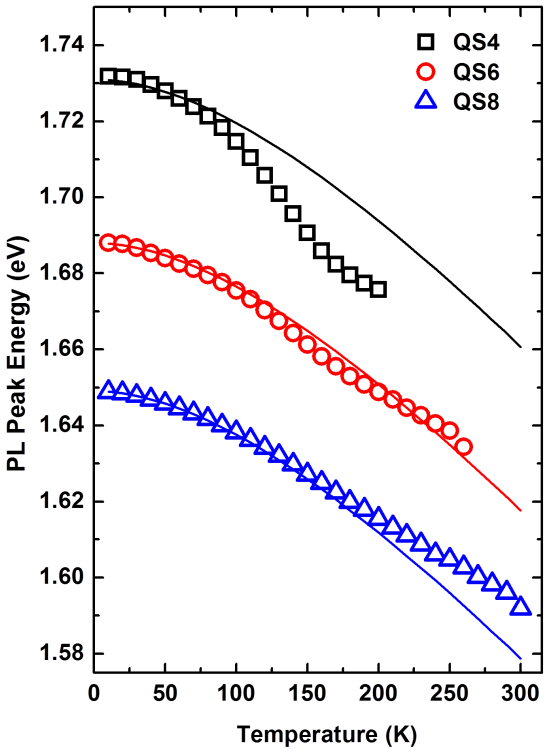

Figure 2. Temperature-dependent PL peak energies of InP/InGaP QS samples (QS4, QS6, and QS8). The solid lines are the calculated bandgap energies obtained by using Varshni's equation with the parameters of bulk InP; $E_g(T)=1.421-4.9\times 10^{-4}T^2/(327+T)$. In order to compare the temperature- dependence of bandgap energies for InP bulk and QSs, at 10 K, the calculated PL peak energy is matched with the measured PL peak energy for each sample.

bulk InP while the $E_g(T)$ for QS6 agrees very well with the measured PL data. Furthermore, QS8 sample shows much smaller bandgap narrowing compared to that of bulk InP at high temperatures. The fast bandgap shrinkage of QS4 is attributed to the increased carrier redistribution from higher energy states (small QDs) to lower energy states (large QDs) via the wetting layer with increasing temperature [10,11,19-21]. The comparable and slower bandgap narrowing of QS6 and QS8, respectively, compared to that of bulk InP can be explained by the enhanced carrier confinement energy due to the increased density and improved shape of QDash with increasing

the MEE cycle.

The PL decay curves for InP/InGaP QS samples measured at the PL peak are shown in Fig. 3 taken at 10 K. The PL decay time at the PL peak is 0.70, 0.51, and 0.46 ns for QS4, QS6, and QS8, respectively. As the MEE growth cycle increases, the PL decay becomes steadily faster. The decrease of decay time with increasing the MEE cycle can be interpreted as being due to the enhanced confinement and the increased wave function overlap among QSs resulted from the increase in the size and density of InP QSs.

Fig. 4 shows the PL decay times and PL spectra of QS4, QS6, and QS8 as a function of emission wavelength measured at 10 K. The PL decay times for QS6 and QS8 increases continuously with increasing emission wavelength while QS4 sample exhibits the longest decay time at around PL peak. The increase of PL decay time with increasing emission wavelength is attributed to the carrier relaxation from higher energy states (smaller QSs) to lower energy states (larger QSs). Byun et al. [10] reported that the PL decay time for InP QSs with InGaP spacer layers of 30 and 50 nm increases with increasing emission wavelength while the PL decay time for InP QS sample with an InGaP spacer of 15 nm increases up to the PL peak and then saturates. The emission wavelength-dependence of the PL decay for InP/InGaP QSs and InAs QDs has been reported by several research groups [9,10,21-23].

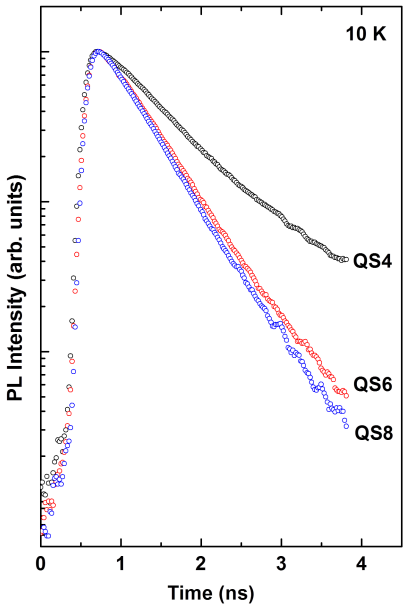

Figure 3. PL decay curves for InP/InGaP QS samples taken at the PL peak energy at 10 K.

IV. Conclusion

InP/InGaP QSs grown by a migration enhanced epitaxy method have been studied by using PL and TRPL measurements. As the MEE growth cycle increases from 2 to 8, the PL peak is redshifted by about 86 nm (213 meV). This redshift is ascribed to the increase in the QS size due to enhanced indium amount with increasing the MEE repetition cycles. As the MEE cycle increases, both the smaller bandgap shrinkages with temperature and the faster PL decays are attributed to the improved confinement as a result of the increased size and density of InP QSs. By changing the MEE growth cycle, the density and size of InP QSs can be controlled and thus the emission wavelength also be controlled.

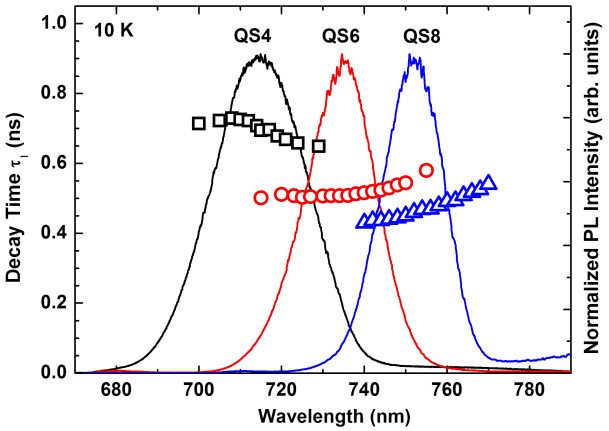

Figure 4. PL decay times for QS4 (open squares), QS6 (open circles), and QS8 (open triangles) as functions of emission wavelength taken at 10 K. The corresponding PL spectra (solid lines) measured at 10 K are also displayed for each sample.

Acknowledgements

This research was supported by the Basic Science Research Program through the National Research Foundation of Korea (NRF) funded by the Ministry of Education, Science and Technology (NRF-2013 R1A1A2A10058310). Time-resolved photoluminescence measurements were performed at the Central Lab of Kangwon National University.

References

[1] M. Sugawara, H. Ebe, N. Hatori, M. Ishida, Y. Arakawa, T. Akiyama, K. Otsubo, and Y. Nakata, Phys. Rev. B, **69**, 235332 (2004).

[2] J. P. Reithmaier, A. Somers, S. Deubert, R. Schwertberger, W. Kaiser, A. Forchel, M. Calligaro, P. Resneau, O. Parillaud, S. Bansropun, M. Krakowski, R. Alizon, D Hadass, A Bilenca, H. Dery, V. Mikhelashvili, G. Eisenstein, M. Gioannini, I. Montrosset, T. W. Berg, M. van der Poel, J. Mork, and B. Tromborg, J. Phys. D: Appl. Phys. **38**, 2088 (2005).

[3] C. Chen, Y. Wang, H. S. Djie, B. S. Ooi, L. F. Lester, T. L. Koch, and J. C. M. Hwang, IEEE J. Sel. Topics Quantum Electron. **17**, 1167 (2011).

[4] D. Zhou, P. E. Vullum, G. Sharma, S. F. Thomassen, R. Holmestad, T. W. Reenaas, and B. O. Fimland, Appl. Phys. Lett. **96**, 083108 (2010).

[5] S. K. Ha, J. D. Song, I. K. Han, D. Y. Ko, S. Y. Kim, and E. H. Lee, J. Korean Phys. Soc. **59**, 3089 (2011).

[6] P. M. Smowton, S. N. Elliott, S. Shutts, M. S. Al-Ghamdi, and A. B. Krysa, IEEE J. Sel. Topics Quantum Electron. **17**, 1343 (2011).

[7] E. Koroknay, W.-M. Schulz, M. Eichfelder, R. Roßbach, M. Jetter, and P. Michler, J. Phys.: Conf. Series, **245**, 012077 (2010).

[8] S. N. Elliott, P. M. Smowton, A. B. Krysa, and R. Beanland, Semicond. Sci. Technol. **27**, 094008 (2012).

[9] R. Rödel, A. Bauer, S. Kremling, S. Reitzenstein, S. Höfling, M. Kamp, L. Worschech, and A. Forchel, Nanotech. **23**, 015605 (2012).

[10] H. R. Byun, M.-Y. Ryu, J. D. Song, and C.-L. Lee, J. Korean Phys. Soc. **66**, 811 (2015).

[11] H. Y. Kim, M-Y. Ryu, and J. S. Kim, J. Lumine. **132**, 1759 (2012).

[12] S. R. Kwon, M.-Y. Ryu, and J. D. Song, Appl. Sci. Converg. Tech. **23**, 387 (2014).

[13] J. W. Oh, H. R. Byun, M.-Y. Ryu, and J. D. Song, J. Korean Vac. Soc. **22**, 92 (2013).

[14] D. Richter, R. Roßbach, W.-M. Schulz, E. Koroknay, C. Kessler, M. Jetter, and P. Michler, Appl. Phys. Lett. **97**, 063107 (2010).

[15] S. Y. Kim, J. D. Song, I. K. Han, and T. W. Kim, J. Nanosci. Nanotech. **12**, 5519 (2012).

[16] P. Podemski, R. Kudrawiec, J. Misiewicz, A. Somers, R. Schwertberger, J. P. Reithmaier, and A. Forchel, Appl. Phys. Lett. **89**, 151902 (2006).

[17] Y.P. Varshni, Physica, **34**, 149 (1967).

[18] M. E. Levinshten, S.L. Rumyantsev, and M. Shur, *Handbook Series on Semiconductor Parameters, Volume 1: Si, Ge, C (Diamond), GaAs,GaP, GaSb, InAs, InP, InSb* (World Scientific, London, 1996).

[19] Y. C. Zhang, C. J. Huang, F. Q. Liu, B. Xu, J. Wu, Y. H. Chen, D. Ding, W. H. Jiang, X. L. Ye, and Z. G. Wang, J. Appl. Phys. **90**, 1973 (2001).

[20] Y-F. Wu, J. C. Lee, T-E. Nee, and J-C. Wang, J. Lumine. **131**, 1267 (2011).

[21] L. M. Kong, J. F. Cai, Z. Y. Wu, Z. Gong, Z. C. Niu, and Z. C. Feng, Thin Solid Films, **498**, 188 (2006).

[22] T. E. J. Campbell-Ricketts, N. A. J. M. Kleemans, R. Notzel, A. Y. Silov, and P. M. Koenraad, Appl. Phys. Lett. **96**, 033102 (2010).

[23] H. J. Lee, M-Y. Ryu, and J. S. Kim, J. Appl. Phys. **108**, 093521 (2010).